Magnetic behavior of antiferromagnetically coupled layers connected by ferromagnetic pinholes

D. B. Fulghum and R. E. Camley
Department of Physics, University of Colorado at Colorado Springs, Colorado Springs, Colorado 80933-7150
(Received 29 June 1995)

The magnetic behavior of a sandwich structure, where two ferromagnetic films are coupled antiferromagnetically across a nonmagnetic spacer film, can be described reasonably well by a simple theoretical model. However, sandwich structures produced experimentally in the laboratory sometimes show behavior not accounted for by this model. These multilayers can exhibit an increased net magnetic moment at low temperatures, as well as a net magnetic moment in the absence of an external field. It has been proposed that the presence of ferromagnetic pinholes could account for some of these features. Our work investigates the temperature-dependent properties of a system with pinholes, and relates this to the size of the pinholes. We also examine some assumptions made in previous work and determine the limits of validity for these assumptions.

I. INTRODUCTION

The magnetic behavior of thin films and multilayers is an important area of research both in solid-state physics as well as in certain industrial fields such as microelectronics. Multilayers are of particular interest as their behavior can differ significantly from any of its components. This behavior varies with the nature of the structure, such as homogeneity, relative spatial arrangements of the different components, and the magnitude and direction of the external field (if any). Generally, the magnetic behavior of homogeneous bulk material is uniform throughout because the vast majority of molecules are buried within the structure, and surface or interface effects can be neglected. In the case of multilayered thin films, however, the number of interface interactions is comparable to that in the bulk. Hence, interface effects must now be taken into account when determining the overall behavior. Usually, these structures are of atomic dimensions (10–200 Å thick), and thus are quite sensitive to small variations in construction or composition. Therefore the conditions under which samples are grown in the laboratory must be carefully controlled, as to insure both layer continuity and spatial uniformity (i.e., thickness, density, etc.). Despite this care, it is clear that real systems have a variety of imperfections. In this paper we address the consequences of one of these imperfections: ferromagnetic pinholes coupling neighboring magnetic films.

A simple magnetic system can be considered as an ordered collection of spins, coupled to one another through magnetic interactions. Coupling is typically ferromagnetic or antiferromagnetic in nature, the former favoring parallel alignment of spins, the latter antiparallel. An important class of magnetic multilayers involves ferromagnetic films which are exchange coupled through a nonmagnetic film. In these structures exchange coupling between spins in different films can be either ferromagnetic or antiferromagnetic, depending on the thickness of the spacer film. The original example of this kind of structure is the Fe/Cr/Fe sandwich,[1] but by now many other material systems have been documented.[2]

The magnetization behavior of the sandwich structure is very different depending on whether the coupling between films is ferromagnetic or antiferromagnetic. For ferromagnetic coupling at low temperatures and in the absence of anisotropy, the net magnetization of the sandwich structure is essentially independent of the external field. All of the spins simply line up in the direction of the field. In contrast, the magnetic properties of two ferromagnetic films coupled antiferromagnetically depend on the presence of an applied external field. Because of the opposing polarizations, a zero net magnetization is predicted at zero external field. In the absence of any anisotropy, the total magnetization should grow linearly with increasing field, until all spins are parallel to one another. As is often the case, theory does not entirely agree with reality: antiferromagnetic bilayers grown in the laboratory are often found to possess a nonzero moment at zero external field.[3–6] Several models have been proposed to explain this discrepancy. Grüberg *et al.* suggested that the usual antiferromagnetic exchange coupling is supplemented by biquadratic coupling.[7] Whereas antiferromagnetic coupling favors diametrically opposed spin moments, biquadratic coupling aligns spin moments perpendicular to the another. A number of physical models have been proposed to explain the origin of this apparent biquadratic coupling. One such model was based on roughness,[8] yet other models indicate that roughness may not be necessary.[9] One recent model has discussed the influence of "pinholes," ferromagnetic bridges connecting the two ferromagnetic films across the interface.[10] As indicated above, the dependence of the magnetization of the entire structure on temperature and external field is of key importance. In the original work on pinholes,[10] the magnetization was calculated in a rigid coupling model where directional variations between individual spins in different atomic layers within a ferromagnetic film were neglected. Also, thermal effects were not considered. Our work is intended to extend this earlier treatment. We do not assume any rigid coupling; each spin is treated on an individual basis. Furthermore we include fluctuations within a local mean-field method which allows us to discuss the temperature dependence of the coupling introduced by the pinhole.

In the course of our discussion, we first establish the analytical structure of the pinhole model, and outline the theory. Two simpler systems, a bulk ferromagnet and two ferromag-

0163-1829/95/52(18)/13436(8)/$06.00

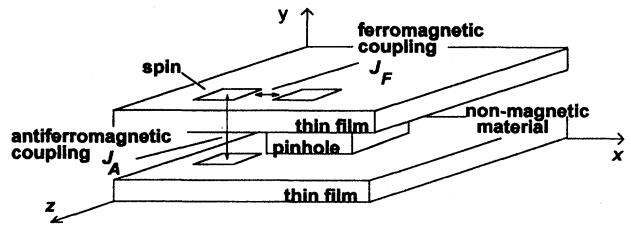

FIG. 1. Basic structure of the pinhole model showing coupling between spins, represented by boxes. Note the nonmagnetic spacer between films. Individual spin orientation is allowed to vary in the xz plane. An external field is applied in the z direction, in the plane of the films.

netic films coupled antiferromagnetically, are then studied for purposes of comparison with later results. This is followed by a discussion of results obtained from the pinhole model, including moment dependence on relative pinhole size and density, and temperature variations. The assumption of rigid coupling was then compared with our model. Finally, the length of the hole was varied, and its effect on the overall net magnetic moment examined.

Our results showed a dependence on the applied field similar to the two antiferromagnetically coupled films: a nearly linear increase in net magnetic moment up to a point of saturation. At a given applied field, however, the net moment for the structure with the pinhole showed a larger magnitude than was observed in the pure antiferromagnetic case at low temperatures. Furthermore, the influence of the pinhole became less significant with increasing temperature. The effectiveness of the pinhole became negligible at a temperature whose value was dependent on the cross sectional area of the hole. This occurred at lower temperatures for smaller holes, where the behavior became that of two antiferromagnetically coupled films. The rigid coupling model yields relatively accurate results if the number of atomic layers in the ferromagnetic film is small, but shows significant error if the number of layers is greater than about four. Finally, longer pinholes between films resulted in lower overall moments, but otherwise behavior was independent of the length.

II. THEORY

The geometry of the pinhole structure is illustrated in Fig. 1. Our model assumes a simple cubic structure. The ferromagnetic films lie in the xz plane and each atomic layer is modeled by a unit cell which contains an $q \times q$ array of spins. Periodic boundary conditions are used in the x and z directions. There are N_f atomic layers in each of the ferromagnetic films. The pinhole which joins the two ferromagnetic films is n_p atomic layers long and is allowed to vary in the cross-sectional area. There is a weak antiferromagnetic exchange J_A between the two films and ferromagnetic exchange J_F between nearest-neighbor spins otherwise.

We note that the pinhole structure may be used to model simpler cases as well. By expanding the pinhole to the same cross-sectional area as the films, we can model a ferromagnetic film. In contrast, if the pinhole is eliminated then we have the case of two ferromagnetic films which are coupled antiferromagnetically at the interface.

Because of the periodic boundary conditions, our structure effectively represents a system of antiferromagnetically coupled films joined by a *density* of pinholes. We can adjust the density of pinholes by changing the size of the unit cell relative to the size of the pinhole.

The theoretical method[11] which we use is an extension of the method applied earlier to transition-metal–rare-earth multilayers[12] and to antiferromagnetic superlattices.[13] Here we briefly review the main points. We use an iterative procedure seeking to find the ground-state structure (spin profile) in which each spin is in equilibrium with the local field imposed by its neighbors. The effective field acting on spin $S_{i,j,k}$ which is at position (i,j,k) is given by

$$\vec{H}_{i,j,k}=H_0\hat{z}+\sum_{a,b,c=\pm 1}\frac{J_{i+a,j+b,k+c}}{g\mu_B}\langle\vec{S}_{i+a,j+b,k+c}\rangle, \quad (1)$$

where H_0 is the external field directed along the z axis, and $\langle S_{i,j,k}\rangle$ denotes the thermal average of the spins as determined by the Brillouin function. We note that one of the "nearest" neighbors for spins at the interface between the magnetic and nonmagnetic films is located across the nonmagnetic spacer film as indicated in Fig. 1.

An iterative procedure is used to obtain the directions and thermal averaged values for the spins. For a given temperature, T, one initially assigns values for the angular direction and magnitude of each spin. Then an individual spin is chosen at random and rotated so as to lie in the direction of its local effective field. This is clearly the minimum energy state for this spin, and so the energy of the entire structure is reduced. The thermal equilibrium magnitude for this spin is then found from

$$\langle S\rangle=SB_s\left(\frac{g\mu_B SH_{\text{eff}}}{kT}\right), \quad (2)$$

where the effective field H_{eff} is given by Eq. (1) and the Brillouin function $B_s(x)$ is given by

$$B_s(x)=\frac{2S+1}{2S}\coth\left[\frac{(2S+1)x}{2S}\right]-\frac{1}{2S}\coth\left[\frac{x}{2S}\right]. \quad (3)$$

A new spin is then chosen and the process is repeated until convergence is achieved, i.e., until a self-consistent final state emerges. By letting the spin system adapt itself to the local field at any particular site in the film, we obtain a spin profile that takes into account the finite structure of the pinhole.

In our work we found that the approximate orientation of all spins was reached within 8000 iterations per spin. Complete convergence to a final state required about 70 000 –80 000 iterations per spin.

III. RESULTS

As an initial check on our three-dimensional iterative method, the ferromagnetic model was compared to known results for a ferromagnetic system with a simple cubic lattice structure. As expected, the self-consistent state was ferromagnetic in character with all spins aligned with the externally applied magnetic field. The temperature dependence was consistent with the results of standard mean-field theory

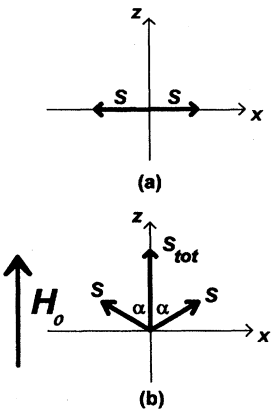

FIG. 2. An antiferromagnetically coupled spin pair in the absence of an external field (a) and the effect of an externally applied field H_0 (b). In (b) the spins are canted with respect to each other with a canting angle 2α.

for uniform systems and the Curie temperature T_C agreed with the standard result

$$T_C=\frac{zJ_FS(S+1)}{3k}, \tag{4}$$

where J_F is the nearest-neighbor exchange coupling, z is the number of nearest neighbors, S is the spin magnitude and k is Boltzmann's constant. Using the fact that the Curie temperature for iron is 1043 K and assuming a spin $S=1$, the ferromagnetic coupling strength J_F was found to be approximately 3.6×10^{-14} erg. We note that because of the periodic boundary conditions the results for the ferromagnet were independent of the size of the unit cell.

An important special case is that of two identical ferromagnetic films which are coupled antiferromagnetically at the interface. This structure, of course, differs significantly from the case of the ferromagnet in a number of respects. In particular, the ferromagnet has a net moment in the absence of an applied field, whereas the antiferromagnetic structure does not. As an external field is introduced, the antiparallel structure is no longer energetically favorable due to the Zeeman energy, resulting in a canted spin state, as is illustrated in Fig. 2. Here we have used $J_A=-0.01J_F$ so that the antiferromagnetic exchange coupling constant J_A is small compared to J_F. In this simplest structure, the canting increases as the external field increases and the net spin moment of the structure increases linearly as a function of the applied field. As the external field is further increased, all the spins eventually lie parallel to the field and the saturation value for the net moment of the structure is obtained.

The net moment of the antiferromagnetically coupled films turns out to be nearly independent of temperature for a fixed applied field. This is a surprising result, yet it can be reasonably well understood by a simple analytical argument. Consider the simple case of two antiferromagnetically coupled moments of equal magnitudes initially along the x axis [Fig. 2(a)]. A field applied along the z axis results in a canted state [Fig. 2(b)], with the net spin magnitude being the vector projection on the z axis:

$$S_{\rm tot}=2S\cos(\alpha). \tag{5}$$

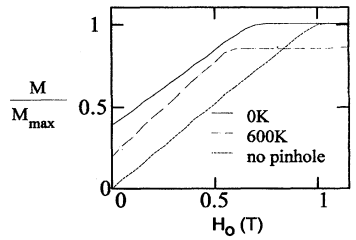

FIG. 3. Field dependence of net moment for temperatures $T=0$ and 600 K. Note the moment is reduced at higher temperatures. Standard parameters are used. For comparison, the magnetic curve for no pinhole ($T=0$) is also shown.

The energy of the system is given by

$$E=J_A(\mathbf{S}_1\cdot\mathbf{S}_2)-g\mu_B\mathbf{H}_0\cdot(\mathbf{S}_1+\mathbf{S}_2) \tag{6}$$

$$=J_AS^2\cos(2\alpha)-2g\mu_BH_0S\cos(\alpha). \tag{7}$$

Minimizing this expression with respect to α, we get

$$\cos(\alpha)=\frac{g\mu_BH_0}{2J_AS}. \tag{8}$$

Substitution of this result back into $S_{\rm tot}$ [Eq. (5)] shows that the net spin magnitude is independent of S, and depends only on the coupling strength and that of the applied field. Strictly speaking this result is only valid at $T=0$, since for $T\neq0$ one would need to calculate the free energy. Nonetheless, we can obtain a feeling for the temperature dependence by replacing S with its thermal average $\langle S\rangle$ in Eqs. (5)–(8). As the temperature is increased, $\langle S\rangle$ is reduced from its maximum value due to thermal fluctuations. As each moment decreases in size, the canting angle also decreases such that the rotation into the field precisely counterbalances the decreasing magnitude. We note that the behavior in a real structure is slightly different from the simple model above because the spin moments inside each film are not rigidly coupled together. As a result, the net moment of the structure in the canted state actually increases slightly with increasing temperature.[11]

The previous discussion serves as a prelude to our main topic—the effect of ferromagnetic pinholes between two antiferromagnetically coupled films. In the absence of the pinhole, the net moment at zero applied field is zero, due to the diametrically opposed moments of the two films. The ferromagnetic bridge provided by the pinhole disrupts this antiparallel structure by inducing a canted state resulting in a net moment at null external field. As the external field is increased at low temperatures, the net moment behaves qualitatively similarly to the antiferromagnet: it increases nearly linearly up to the point of saturation. At higher temperatures the transition to saturation occurs at a much lower applied field. As the temperature is increased, the thermally averaged spin moment decreases, particularly at the interfaces. As a result, antiferromagnetic exchange energy decreases, and a smaller external field is required to align the spin moments in the direction of the field. This also results in a smaller overall net moment. Figure 3 illustrates this for the special case where the two films consisted of $N_f=4$ atomic layers each, separated by $n_p=3$ atomic layers of nonmagnetic material. The pinhole bridging the two films was a 2×2 subcell of a

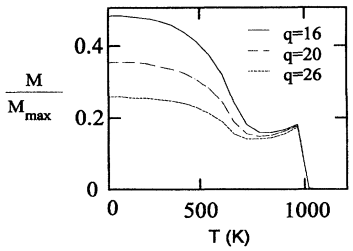

FIG. 4. Effect of different pinhole densities on net moment temperature dependence. The parameters $q=16$, 20, 26 correspond to pinhole densities of 1.6, 1.0, and 0.6 %, respectively. $H_0=0.1$ T.

16×16 array, corresponding to a pinhole density of 1.6% (by cross-sectional area). We also continue to use $J_A=-0.01J_F$. These conditions will hereafter be referred to as standard parameters, any variations of which will be explicitly noted.

The effect of the pinhole on the temperature dependence is somewhat more dramatic as can be seen in Fig. 4. Here we plot the magnetic moment of the structure as a function of temperature when an external field of 0.1 T is applied. At low temperatures the presence of the ferromagnetic bridge favors a considerably larger moment that would normally be present at a given applied field due to canting. As the temperature increases, the net moment decreases gradually at first, then rapidly, to a point where it is nearly constant. Finally, as the Curie temperature is approached, the net moment drops off sharply to zero.

Different pinhole densities were modeled by varying the $q\times q$ unit-cell dimensions while keeping the pinhole dimensions constant at 2×2. The results obtained when $q=16$, 20, or 26, corresponding to densities of 1.6, 1.0, or 0.6 %, respectively, are shown in Fig. 4. The overall magnitude of the moment decreases with smaller pinhole densities, as the ferromagnetic influence of each pinhole is overwhelmed by the antiferromagnetic coupling between films. Note that the temperatures where phase changes occur remain the same for all cases. As before, the model was analyzed assuming standard parameters, excepting the unit-cell dimensions.

The influence of the pinhole on the net magnetic moment is strongly temperature dependent. This is a direct result of the finite dimensions of the pinhole. In pinholes of smaller cross section, a larger number of spins are located at the sides of the pinhole. These spins see a smaller effective field than those in the bulk because they have fewer magnetic neighbors. Since the thermally averaged moment depends on the local effective field, the spins on the side of the pinhole have a smaller averaged moment than those in the bulk for a given temperature. As a result, the magnetization in the pinhole is extinguished at a significantly lower temperature than that in the bulk. The vanishing of the pinhole results in the initial rapid drop in the net magnetization of the structure as seen in Fig. 4. When the ferromagnetic influence of the pinhole is no longer significant, the net moment behaves as in the simple model of two films which are antiferromagnetically coupled. As pointed out previously, the net moment in this structure is nearly temperature independent. The reason for the slight increase in moment seen in Fig. 4 at higher temperatures is discussed in Ref. 11.

We explore the temperature dependence of the magnetization on the size of the pinhole further in Figs. 5–7. In Fig. 5(a) we consider pinholes of different cross sections but with the pinhole density kept constant. The key difference between the structures is that the number of nearest neighbors depends on the details of the pinhole cross sectional structure. For example in a 2×2 pinhole each spin in the pinhole has four nearest magnetic neighbors. In contrast each spin in a 2×1 pinhole has only three nearest magnetic neighbors. This leads to a smaller effective field for the 2×1 case and as a result a rapid decrease in magnetization occurs at a lower temperature for the smaller pinholes. It is interesting to note that in Fig. 5(a), where the pinhole density is kept constant, the values for the magnetization at high and low tem-

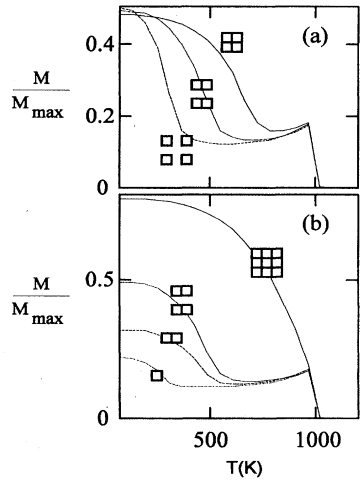

FIG. 5. Effect of different pinhole sizes and structures on the temperature dependence of the magnetization using standard parameters ($H_0=0.1$ T). In (a) the pinhole structure is varied in such a way so that the density of pinholes remains the same. In (b) the density of pinholes is allowed to vary. The cross sectional shape of the individual pinholes is shown for each curve.

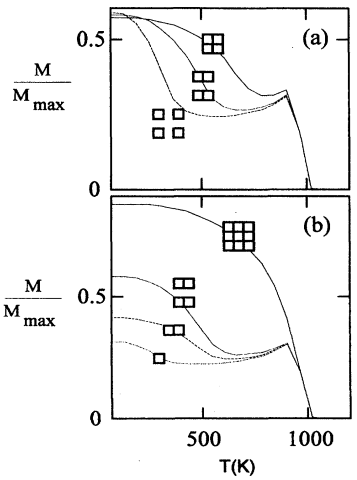

FIG. 6. Effect of an increased external field ($H=0.2$ T) on the magnetization for different pinhole sizes and structures. Variations in pinhole structure are shown in (a), while different pinhole densities are shown in (b). The cross sectional shape of the individual pinholes is shown for each curve.

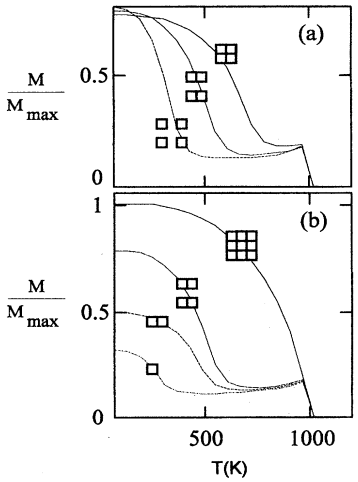

FIG. 7. Effect of different pinhole sizes and structures on the temperature dependence of the magnetization in a reduced external field. Both the field and antiferromagnetic coupling are reduced by a factor of 2 compared to standard parameters. Again, the dependence of different pinhole structures (a) and densities (b) are shown. Each pinhole shape is shown for each curve.

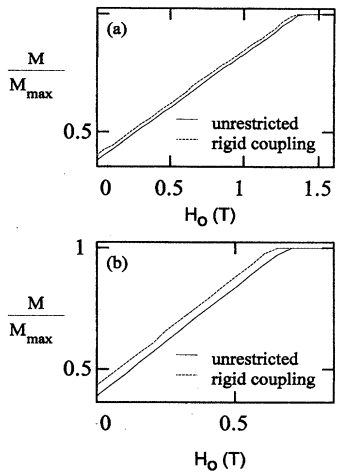

FIG. 8. Comparison of general model (solid line) to the rigid coupling approximation (dotted line) for (a) two layers per film (b) four layers per film. The rigid approximation models the system relatively well at two layers, but is significantly worse at four layers.

peratures are the same for each structure, and the main difference between the curves is where the sharp drop in magnetization occurs.

In Fig. 5(b) we examine results for pinholes with different cross sections, but here the pinhole density is not constant. We see that by the time the pinhole density is 3.5% (the 3×3 structure) the antiferromagnetic coupling between the layers is overcome and the structure simply acts like a ferromagnet. When we compare the results for the two systems with 2×1 structures, we see that the temperature dependence is approximately the same, i.e., the magnetization starts to decrease at about the same temperatures and levels off at about the same temperatures.

In Fig. 6 we again show magnetization as a function of temperature for a variety of pinhole structures. The external field is doubled compared to Fig. 5. In comparing Figs. 5 and 6 we see that the magnitude of the magnetization is increased for the higher field but that the thermal dependence is essentially unchanged. This is to be expected because the thermal behavior depends mostly on the effective exchange field which is much larger than the external field.

In Fig. 7 we investigate the effect of changing the antiferromagnetic exchange coupling between the films. Compared to Fig. 5 we have reduced both the magnetic field and the antiferromagnetic coupling by a factor of 2. In the absence of a pinhole this would result in the same canting angle in both cases since, as seen in Eq. (8), the canting angle depends on the ratio H_0/J_A. However with the pinhole included we see that magnetization is significantly enhanced for Fig. 7 as compared to Fig. 5. The reason for this is that the pinhole is simply much more effective in its effort to produce a ferromagnetic alignment when J_A is small. We note that the thermal behavior is only slightly changed, confirming the idea that the thermal behavior is basically dependent on the cross-sectional structure and not on other factors.

Previous work on pinholes in antiferromagnetically coupled thin films invoked several assumptions in order to simplify the problem. One assumption was that the spins within an atomic layer of the thin ferromagnetic film were essentially rigidly coupled to the spins above and below that layer. Thus no differences in orientation were allowed from one atomic layer to the next. This allows one to model the thin ferromagnetic film as being composed of one layer only, but with exchange and Zeeman energies proportional to the thickness of the film. Subject to this assumption, the effective field is now given by

$$\mathbf{H}_{i,j,k}=N_f H_0\hat{z}+N_f\sum_{a,b=\pm1}\frac{J_{i+a,j+b,k}}{g_n\mu_B}\langle\mathbf{S}_{i+a,j+b,k}\rangle + \sum_{m=\pm1}\frac{J_{i,j,k+m}}{g_n\mu_B}\langle\mathbf{S}_{i,j,k+m}\rangle, \tag{9}$$

where N_f is the number of atomic layers within a ferromagnetic film.

Of course, as the thickness of the ferromagnetic films is increased there will be some variation of the orientation of the spins from one atomic layer to the next. We can test the validity of the "rigid coupling model" with our approach since it allows the moments in each atomic layer to vary independently. In Fig. 8 we plot the net moment of the system in the direction of the applied field as a function of the external field. We see that the net moment was modeled relatively well by the rigid coupling approximation for two layers [Fig. 8(a)], but grew increasingly worse as more layers were considered. In particular, the apparent saturation field is significantly different for the four layer film when compared to the rigid coupling results as can be seen in Fig. 8(b).

We explore in detail the variation in both the saturation and null moment field as a function of the number of layers N_f for both models. The results, calculated for standard parameters, are shown in Fig. 9. Note that in both cases the two curves coincide for $N_f=1$ (as they should), but grow farther apart as N_f increases. In particular, the null field moment shows a 5.5% error at $N_f=2$, but a 16.5% error at $N_f=8$

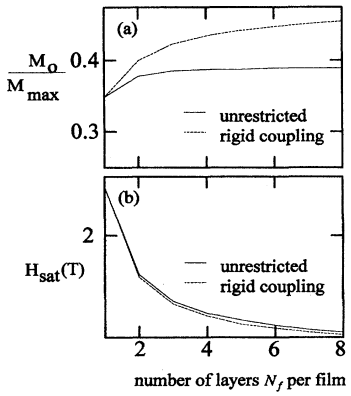

FIG. 9. Variation of the null field moment (a) and saturation fields (b) as a function of the thickness N_f of each film. Both the rigid coupling and the unrestricted models are shown. Standard parameters are used in both cases ($T=0$). Note the significant percent error at high N_f.

[Fig. 9(a)]. Similarly, the apparent saturation field shows a 3% error at $N_f=2$, but a 14.3% error at $N_f=8$ as shown in Fig. 9(b).

We note also that the rigid coupling approximation automatically excludes the possibility that the thermal averaged magnitude of the spins can vary from layer to layer. Such a variation occurs naturally when the temperature is near the transition temperature for the film. While this might only be of academic interest in Fe/Cr/Fe structures, since the transition temperature is on the order of 1000 K, it will certainly be important in other layered compounds such as Gd/Y/Gd where the transition temperature is about 280 K.[14]

We can obtain some additional insight into the difference between our general model and the rigid coupling model by examining the angular positions of individual spins in each layer. For this comparison we use our standard parameter with a 2×2 pinhole centered on a 16×16 array, subject to an external field of 0.1 T. Each film is $N_f=4$ layers thick, separated by $n_p=3$ layers of nonmagnetic material bridged by the pinhole. The details of the structure are shown in Fig. 10. Spin arrangements in the top film were examined, as well as those within the pinhole itself.

When spin orientations are allowed to vary individually, significant differences between layers result. Figure 11 shows the 6×6 grid centered on the pinhole. Figure 11(a) shows the spin orientations in layer 4, which is adjacent to the pinhole. Here we see significant differences between the angular position of spins within the layer. Note particularly the differences in spin direction immediately above the pinhole in Fig. 11(a). Spins outside the pinhole show very small deviations. The spin map of layer 1 is shown in Fig. 11(b). Note that this layer if farthest from the pinhole, and in contrast to layer 4 shows almost negligible differences between the orientations of individual spins. The region directly above the pinhole is represented by a dotted box in both figures.

It is interesting to note that the average spin angle (as measured from the magnetic field) in each layer shows only small deviations from layer to layer. In our example, the average angle in layer 4 [adjacent to the pinhole; Fig. 11(a)] is approximately 59°. Farthest from the pinhole, in layer 1 [Fig. 11(b)] the average angle if 61°. Angular differences between adjacent spins within a given layer are even smaller. This results from the relatively strong ferromagnetic exchange coupling between spins. While angular variations *between* spins are small, the entire system is canted away from the most energetically favorable orientation in the absence of the pinhole, diametrically opposed spins across the interface. Recall that the antiferromagnetic coupling constant J_A is a small fraction of the ferromagnetic coupling constant J_f, and consequently has a smaller impact on the energy. As a result, it is less costly to disrupt the antiferromagnetic coupling between spins across the interface than the ferromagnetic coupling between adjacent spins. We estimate that the effect of the pinhole is felt at least 15–20 lattice sites away.

Within an atomic plane of the pinhole all spins point in the same direction. However, the deviation from plane to plane within the pinhole can be quite large, forming a "twist" between films. For example, the spin angles as measured from the magnetic field in the top and bottom layers of the pinhole are $+27°$ and $-27°$, respectively, whereas the middle layer is in line with the external field (as one might expect from symmetry). Spin orientations in the lower film are symmetric with respect to their counterparts in the upper film.

The net magnetic characteristics are also dependent on the

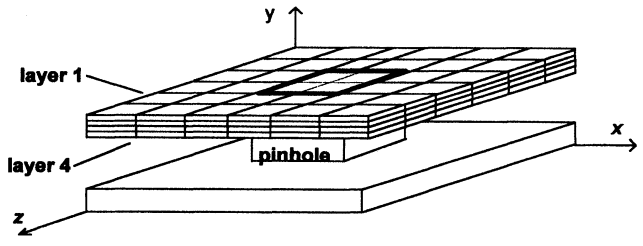

FIG. 10. Pinhole model showing spatial arrangements of spin layers 1 and 4 relative to the pinhole. The pinhole cross section is shown by the heavy black box.

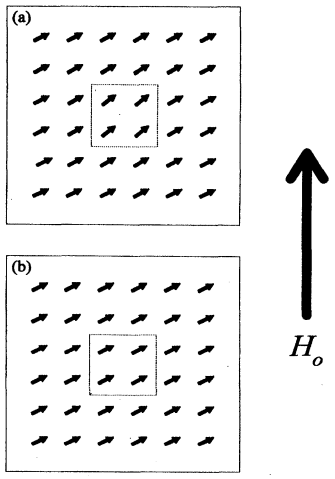

FIG. 11. Spin maps for layer 4 (a) and layer 1 (b). This data was taken assuming standard parameters, at $T=400$ K in an external field H_0 of 0.1 T. The cross section of the pinhole is represented by a dotted box.

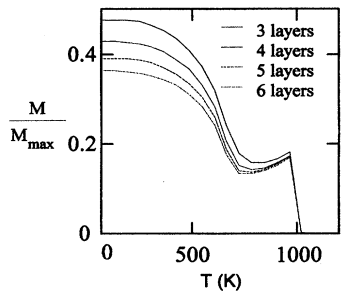

FIG. 12. Temperature dependence of the magnetization for different length pinholes. The qualitative behavior is similar for all temperatures. Note the differences in overall moment as the number of layers is increased.

distance between the films and hence on the length of the pinhole. This is explored in Fig. 12 where we plot magnetization as a function of temperature for pinholes of different length. We use our standard parameters except we vary the pinhole length. The qualitative behavior of the system remained the same. The overall magnitude of the moment, however, decreased as the length of the pinhole was increased. The pinhole can be thought of as a torsional spring acting between two antiferromagnetically coupled films. As the spring becomes longer, it is easier to twist around its axis. In the same manner, longer pinholes are more readily twisted by the antiferromagnetic forces between the films, resulting in a smaller net moment. The reason it is easier to twist longer pinholes is that the angular difference between atomic layers is smaller for longer pinholes. For example, the pinhole which is six layers longer has angular *differences* between layers on the order of 18°, as opposed to 27° for the four layer pinhole. Therefore, the cost of the twist in ferromagnetic exchange energy within the pinhole is reduced.

IV. CONCLUSION

Through computer modeling we have shown that the existence of ferromagnetic pinholes in multilayer thin-film structures play a significant role in magnetic properties. Specifically, pinholes connecting two ferromagnetic films coupled antiferromagnetically were analyzed under various conditions. The model was subject to different external parameters, such as temperature T and applied field H_0, as well as internal factors, including pinhole density, cross-sectional area, and length. An approximation of rigid coupling between layers was also evaluated, in order to determine the range of validity.

Field dependence of the net moment was found to be qualitatively similar at all temperatures, increasing nearly linearly from a nonzero value to a point of saturation. At higher temperatures, the overall moment was smaller and saturation was reached at smaller fields. The pinhole effectively provides a boost to the net moment at low temperatures, the size of which is related to the pinhole density. As the temperature is increased, the pinhole is effectively eliminated and the behavior approaches that of two antiferromagnetically coupled films. The temperature where the pinholes vanish due to thermal fluctuations was found to be independent of pinhole density, but depends strongly on the cross-sectional area of each hole.

The assumption of rigid coupling was valid at low temperatures, but because it does not allow for thermal variations within a layer, fails at higher temperatures. An examination of the individual spin orientations showed differences *between* spin orientations near the hole to be significant, while those farther away were negligible. Since the entire structure is canted by the pinhole, this results in a large healing distance. Pinhole influence was also found to be length dependent, with longer pinholes being less effective.

Our model assumed a uniform pinhole density as a consequence of periodic boundary conditions, whereas in reality such a distribution would be entirely random. It is not expected that this invalidates the above results, because it is the net result of this density that is observed experimentally. Random spatial variations on an atomic scale, when viewed from a relatively macroscopic scale, will, on the average, appear uniform.

Finally, we note that this work neglects the influence of cubic anisotropy and thus the results are directly applicable to systems such as NiFe/Ag which shows only minimal anisotropy. However, cubic anisotropy is important in some systems, Fe/Cr for example. The influence of such anisotropy on magnetization curves as a function of magnetic field can be substantial as can be seen in both experimental[4,7] and theoretical work.[15] However, anisotropy fields are small compared to typical ferromagnetic exchange fields. As a result, the thermal dependence of the magnetization, which in this model depends primarily on the ferromagnetic exchange within the multilayer, will be very similar to that calculated here even for systems with in-plane anisotropy.

ACKNOWLEDGMENT

This work was supported by the U.S. ARO under Grant No. DAAH 04-94-G-0253.

[1] P. Grünberg, R. Schreiber, Y. Pang, M. B. Brodsky, and H. Sowers, Phys. Rev. Lett. **57**, 2442 (1986).

[2] S. S. P. Parkin, N. More, and K. P. Roche, Phys. Rev. Lett. **64**, 2304 (1990).

[3] J. M. George, L. G. Pereira, A. Barthélémy, F. Petroff, L. Steren, J. L. Duvail, and A. Fert, Phys. Rev. Lett. **72**, 408 (1994).

[4] B. Heinrich, Z. Celinski, J. F. Cochran, A. S. Arott, K. Myrtle, and S. T. Purcell, Phys. Rev. B **47**, 5077 (1993).

[5] C. J. Gutierrez, J. J. Krebs, M. E. Filipkowski, and G. A. Prinz, J. Magn. Magn. Mater. **116**, L305 (1992).

[6] J. Unguris, R. J. Celotta, and D. T. Pierce, Phys. Rev. Lett. **67**, 140 (1991).

[7] P. Grünberg, S. Demokritov, A. Fuss, R. Schreiber, J. A. Wolf, and S. T. Purcell, J. Magn. Magn. Mater. **104-107**, 1734 (1992).

[8] J. C. Slonczewski, Phys. Rev. Lett. **67**, 3172 (1991); see, also, J. C. Slonczewski, J. Appl. Phys. **73**, 5957 (1993) for a recent review of a variety of different mechanisms for biquadratic exchange.

[9] J. Barnas and P. Grünberg, J. Magn. Magn. Mater. **121**, 326 (1993).

[10] J. Bobo, H. Fischer, and M. Piecuch, in *Magnetic Ultrathin Films: Multilayer and Surfaces/Interfaces and Characterization*, edited by B. T. Jonker, S. A. Chambers, R. F. C. Farrow, C. Chappert, R. Clarke, W. J. M. de Jonge, T. Egami, P. Grünberg, K. M. Krishnan, E. E. Marinero, C. Rau, and S. Tsunashima, MRS Symposia Proceedings No. 313 (Materials Research Society, Pittsburgh, 1993), p. 467; J. F. Bobo, M. Piecuch, and E. Snoeck, J. Magn. Magn. Mater. **126**, 440 (1993).

[11] See the review article by R. E. Camley and R. L. Stamps, J. Phys. Condens. Matter **5**, 3727 (1993).

[12] C. Dufour, Ph. Bauer, M. Sajieddine, K. Cherifi, G. Marchal, Ph. Mangin, and R. E. Camley, J. Magn. Magn. Mater. **121**, 300 (1993).

[13] A. S. Carrico and R. E. Camley, Phys. Rev. B **45**, 13 117 (1992).

[14] J. Kwo, M. Hong, F. J. Di Salvo, J. V. Waszczak, and C. F. Majkrzak, Phys. Rev. B **35**, 7925 (1987).

[15] A. S. Carrico, D. R. Tilley, and R. E. Camley, Solid State Commun. **94**, 299 (1995).